SME Annual Meeting
Feb. 24 - 27, 2018, Denver, CO

Preprint 19-076

A CASE-STUDY OF ROOF SUPPORT ALTERNATIVES FOR DEEP COVER ROOM-AND-PILLAR RETREAT MINING USING IN-SITU MONITORING AND NUMERICAL MODELING

G. Rashed, CDC NIOSH, Pittsburgh, PA
M. Sears, CDC NIOSH, Pittsburgh, PA
J. Addis, CDC NIOSH, Pittsburgh, PA
K. Mohamed, CDC NIOSH, Pittsburgh, PA
J. Wickline, Coronado Coal, Charleston, WV

ABSTRACT

To better understand the load shedding and the stress transfer on coal pillars due to room-and- pillar retreat mining in deep cover panels, researchers from the National Institute for Occupational Safety and Health (NIOSH) conducted a monitoring field study. Two sites, at overburden depths of 1,000 ft (304.8 m) and 1,500 ft (457.3 m), were selected in a room-and-pillar mine operating in Southern West Virginia. The deformation and stress changes in the roof and two adjacent pillars at each site were monitored during the retreat mining process. The monitoring results and field observations were used to calibrate large-scale FLAC3D models for each site. The calibrated models were used to assess different sizes of roof bolts installed in deep cover areas.

INTRODUCTION

Deep cover room-and-pillar retreat mining is an important emerging issue that will intensify in the future as shallower reserves are depleted (Mark, 2009; Chase et al., 2002). During pillar retreat mining, the likelihood of local and/or global instabilities increases due to elevated stress levels near the pillar line because of the abutment loading. In the last decade, approximately 31% of the room-and-pillar mining groundfall fatalities in the United States occurred during pillar retreat mining. Between 2013 and 2017, this proportion increased to 55%, of which 50% of these fatalities were due to falls of roof and rib that occurred during pillar recovery (MSHA, 2018).

One interesting piece of information about pillar recovery fatalities was that the victim was nearly always under bolted roof. Sheared and broken #5 (5/8-in), fully grouted rebar bolt failure contributed to three of four fatal roof fall incidents that have occurred in deep cover retreat mines (NIOSH, 2010). This claim raised the following question at the study mine: Is it safe to use a 4-ft long #5 (5/8-in) rebar bolt grade 60 at a depth of cover more than 1,000 ft (304.8 m)? There was some concern about shear failure of the #5 (5/8-in) rebar bolt at a depth of cover over 1,000 ft (304.8 m).

To answer the question and to reduce accidents and fatalities caused by ground falls due to room-and-pillar retreat mining in deep cover panels, the National Institute for Occupational Safety and Health (NIOSH) monitored the roof and rib deformation and the change in vertical pressure within two adjacent pillars during pillar recovery. The study was conducted at two deep cover sites in a room-and-pillar mine located in Southern West Virginia that operates in the Lower War Eagle (LWE) seam. The monitored sites were selected at 1,000 ft (304.8 m) and 1,500 ft (457.3 m) depths of cover. In this paper, site-1 represents the monitored site at 1,000 ft (304.8 m) of cover, while site-2 represents the monitored site at 1,500 ft (457.3 m) of cover.

For this study, large-scale FLAC3D numerical models were calibrated based on both field observations and instrumentation results. The calibrated models were then used to compare the ground response and the induced stresses of two pillars at instrumented sites 1 and 2. The maximum lateral displacement (roof shift) obtained from the calibrated large-scale FLAC3D models was applied to a small-scale FLAC3D bolted models, the safety factor for axial stresses of the simulated roof bolts was calculated at the deep cover sites.

GEOLOGICAL CONDITIONS

Obtaining accurate geologic information is required to predict meaningful deformation and stresses from the numerical models. The typical geology from boreholes near the instrumented sites consists mainly of interbedded shale, sandy shale, silty shale, and sandstone. Additionally, the roof was scoped to provide a better understanding of the local geology at the instrumented sites. Tables 1 and 2 show the scoped rock type up to a distance of 20 ft (6.0 m) into the roof at site-1 and site-2, respectively. The stratigraphic columns from the drill holes at other locations obtained from the mine indicate that the immediate roof strata matches well the stratigraphic column from the scope holes.

Table 1. Immediate roof rock-type at site-1.

Depth, ft	Rock type
0.7–roofline	Thinly bedded silty shale
0.7	Bed separation
2.8–0.7	Thinly bedded clayey shale with coal streaks
16.8–2.8	Thinly bedded silty shale, sharp contact
20–16.8	Thinly bedded sandy shale with sandstone streaks, gradational lower contact

Table 2. Immediate roof rock-type at site-2.

Depth, ft	Rock type
8.5–roofline	Thinly bedded clayey shale
13–8.5	Thinly bedded silty shale, gradational lower contact
15.5–13	Thinly bedded silty shale with coal streaks, gradational lower contact
19–15.5	Sandy shale with thinly bedded sandstone streaks
20–19	Fine grained sandstone with thinly bedded shale streaks

GEOTECHNICAL PARAMETERS

Underground geotechnical data on the immediate roof rock and the coalbed were collected. They are among the input parameters required to generate the large-scale FLAC3D numerical models for the instrumented sites. Obtaining the appropriate input material properties required testing of small-scale coal and rock specimens and then scaling the small scale strength parameters to obtain a reasonable in-situ strength parameters. Coal blocks were obtained from coal ribs during underground site investigations. Unconfined Compressive Strength tests (UCS) were conducted on the specimens using a Tinius-Olsen testing machine. Table 3 summarizes sample dimensions and the UCS results. The UCS of coal is an input parameter in the coal-mass model used to simulate the coal seam Mohamed et al. (2015). Additionally, the point load strength index was conducted for coal specimens from the LWE seam and a good correlation was found between the UCS of coal and the point load strength index (Rashed et al., 2018). The UCS of the shale, sandy shale, and sandstone found in the roof and floor strata were determined and the results were provided by the mine. The average UCS for the shale and sandy shale was

5,677 psi (39 MPa) and 9,455 psi (65 MPa), respectively, while the UCS for sandstone was 22,145 psi (152.7 MPa).

Table 3. Summary of the UCS and Young's modulus for coal specimens from LWE coal seam.

specimen #	Length, in	Width, in	Height, in	W/H ratio	UCS, psi	E, psi
1	3.47	3.87	3.29	1.1	1,762	269,489
2	3.45	3.5	3.60	1.0	1,946	264,984
3	3.95	4.5	3.94	1.1	1,607	243,887
4	2.87	2.40	3.62	0.7	3,060	290,000
5	2.84	2.91	3.342	0.9	3,252	320,100
6	1.84	1.8	3.621	0.5	1,905	260,500

MINING CONDITIONS

The mine produces bituminous coal from the LWE seam by the room-and-pillar retreat mining method. Site-1 and site-2 were located in the #6 entry in the 3rd Left Panel. The panel width was subcritical and consists of eight entries and included barrier pillars between the subsequent panels. The dimensions of the pillars are approximately 53 ft (16.1 m) x 99 ft (30.1 m) rib-to-rib (R-R). The entries and crosscuts were about 20 ft (6.0 m) wide at the instrumented sites. Site-1 was located between crosscuts 9 and 10, while site-2 was located between crosscuts 21 and 22. The mining height is approximately 5.2 ft (1.6 m) at the instrumented sites. There was neither sudden topographic changes nor multiple seam interaction in the 3rd left panel.

During retreat mining, two continuous miners (CMs) are used simultaneously to extract each row of pillars. In this method of pillar extraction, mining progresses from the center of the panel outward in a staggered fashion. This method results in leave blocks that are left unmined in the center of the panel rather than on the sides. The number of these blocks in the panel corresponds to a panel width providing adequate pillar stability for a given depth of cover. In this case, one line of pillars is left unmined in the center of the panel at Site-1, while two lines of pillars are left unmined at the center of the panel at site-2. Figure 1a and b show the pillar layout and extraction sequence at site-1 and site-2, respectively. Barrier pillars are used to isolate the active panels from the previous gob.

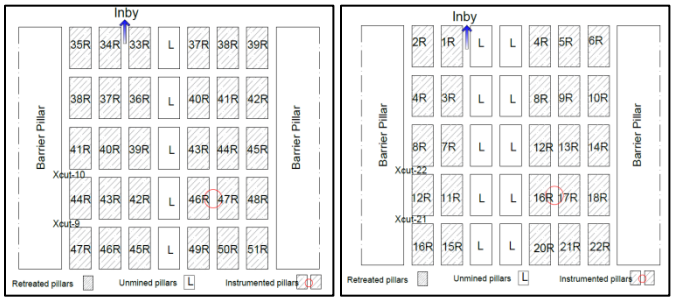

a. Site-1 b. Site-2

Figure 1. Pillar retreat plan for a) site-1 and b) site-2. Instrumented sites were marked by red circles.

Reducing the panel width by leaving unmined pillars at the center of the panel designed to reduce the elevated stresses of the abutment loading during pillar retreat mining, particularly under deeper cover. No slab cuts were taken from the barrier and a final stump was left unmined to provide roof support during pillar recovery. The size of the final stump was a minimum 6 ft (1.8 m) x 6 ft (1.8 m).

Six wood posts are spaced 3-4 ft apart across the entry to provide support before a pillar lift was started. 8-ft (2.4-m) long cable bolt was used as a supplemental support in the intersection areas, the spacing between the cable bolts is approximately 6 ft (1.8 m). The mine is using one row of 3-ft (0.9-m) long #5 (5/8-in) fiberglass bolts to support the coal pillar ribs in areas greater than 1,000 ft (304.8 m) of overburden. The spacing of rib bolts at site-2 is roughly 8 ft (2.4 m).

VISUAL OBSERVATIONS

Underground visual observation was one of the primary techniques used to evaluate the stress and deformation levels at the instrumented sites. Observational data can provide information about large areas of a mine and, when combined with instrumentation results, can be used to validate large-scale FLAC3D models. When the pillar line was located at the instrumented sites, the immediate roof, floor, ribs, and the extent of roof caving were observed in the retreated panel.

At both site-1 and site-2, there were no signs of the following: excessive roof sagging, open fractures in the roof, roof cutters near the ribline, or outby roof failure. Also, there were no signs of excessive roof bolt deformations, such as excessive bolt elongation or severely deformed bolt-plates. The floor was not visibly heaved, and it was in good condition. In other words, the structural integrity of the immediate roof and floor was sufficient to withstand development stresses and retreat mining induced abutment stresses at both site-1 and site-2. The entry between the two instrumented pillars at each site was accessible and the ribs were in good condition with little rib spalling.

In addition to the visual observation and evaluation, several test holes were drilled in the roof near the instrumented sites to evaluate the immediate roof for bedding separations and the lateral displacement/roof shifting. No roof shifting was recorded at either site test holes. However, roof bedding separation was reported at site-1 (see Table-1).

At site-1, the immediate roof caved right behind the pillar line with no signs of roof overhanging, and the gob generally formed quite rapidly. However, at site-2 prior to the removal of the data logging system, the immediate roof did not cave, and was overhanging for at least one break, approximately—100 ft (30.4 m) inby the instrumented pillars. The narrowness of the panel width for site-2 and the presence of sandstone and silty shale in the roof (see Table 2) may have restricted caving.

INSTRUMENTATION PLAN AT SITE-1 AND SITE-2

Instruments have been used increasingly in mines to measure deformation, stress, strain, and load. Such measurements serve two purposes. First, they provide quantitative information about the mechanics of stability and in aiding engineering decisions. Second, they can be a useful tool in addition to field observations for calibrating numerical models (Larson et al., 2000; Klemetti et al., 2017). Monitoring systems can warn mine staff of impending ground control failures or hazardous working conditions (Thomas, 2015). The monitoring was performed in two adjacent pillars within the #6 entry at site-1 and site-2. For site-1, all instruments were located between crosscuts 9 and 10. For site-2 they were located between crosscuts 22 and 23. Figure 2 shows a schematic for the instrument type and location at both site-1 and site-2. All instruments were installed after the panel was developed. Hence, pillar-retreat mining will be the main cause for any change in movement or loading that occurs in the roof, rib, or pillar.

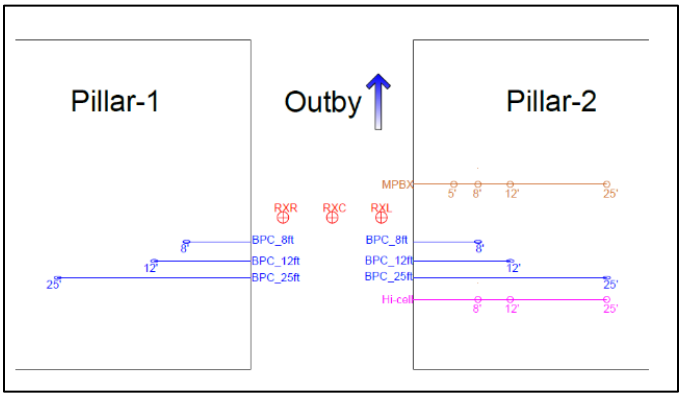

Figure 2. Instrument type and location for both site-1 and site-2.

For each instrumented site, the instruments included were: one 4-point roof extensometer (RXC), two 6-point roof extensometers (RXL and RXR), one borehole multi-point rib extensometer (MPRX), six borehole pressure cells (BPCs), and three hollow inclusion cells (Hi-cells). The Hi-cells were installed into the roof near the rib at 45º

angles. The RXC, placed in the middle of the entry, had anchors located 25 ft (7.6 m), 13 ft (3.9 m), 9 ft (2.7 m), and 5 ft (1.5 m) above the roof line, while RXL and RXR, placed four feet away from the RXC, had anchors located 13 ft (3.9 m), 10 ft (3.0 m), 8 ft (2.4 m), 6 ft (1.8 m), 4 ft (1.2 m), and 2 ft (0.6 m) above the roof line. The MPRX had anchors located 25 ft (7.6 m), 14 ft (4.2 m), 8 ft (2.4 m), and 5 ft (1.5 m) into the pillar. The BPCs were located 25 ft (7.6 m), 12 ft (3.6 m), and 8 ft (2.4 m)) from the pillar rib. Three BPCs were installed in instrumented pillar-1 and three BPCs were installed in pillar-2 (see Figure 2).

INSTRUMENTATION RESULTS

Pressure Change in Borehole Pressure Cells (BPCs)

Figure 3 shows the pressure change in the BPCs in instrumented pillars-1 and 2 at site-1. The pressure change in the BPC represents the induced abutment load due to only pillar retreat mining. The maximum pressure change in the BPCs is roughly 500 psi (3.4 MPa). As shown in Figure 3-a, the pressure change in BPC-12ft is higher than the pressure change in BPC-8ft. One potential explanation for this could be that BPC-8ft was tilted during field installation, and hence the measured change in pressure represented a fraction of the increased vertical load.

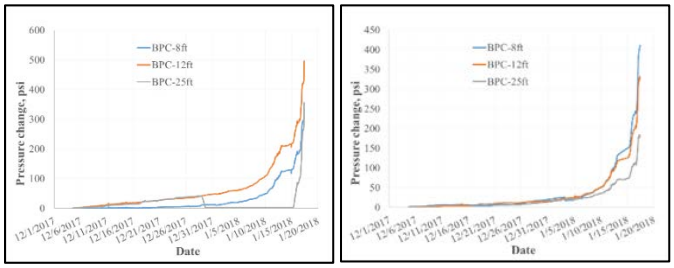

a. Pillar-1 b. Pillar-2

Figure 3. Pressure change in the BPCs for a) pillar-1 and b) pillar-2 at site-1.

Figure 4 shows the pressure change in the BPCs in the instrumented pillar-1 at site-2. Although, the BPCs in pillar-2 appeared to be functioning, they failed to collect data due to an electronics malfunction. The maximum pressure change in the BPCs in pillar-1 is approximately 2,752 psi (18.9 MPa). The strength and stiffness of the immediate and main roof beams may have inhibited gob formation and caving at site-2. The caving characteristics of the immediate roof has the potential to result in a significant impact on stress levels at the pillar line at site-2 during room-and-pillar retreat mining due to poor caving.

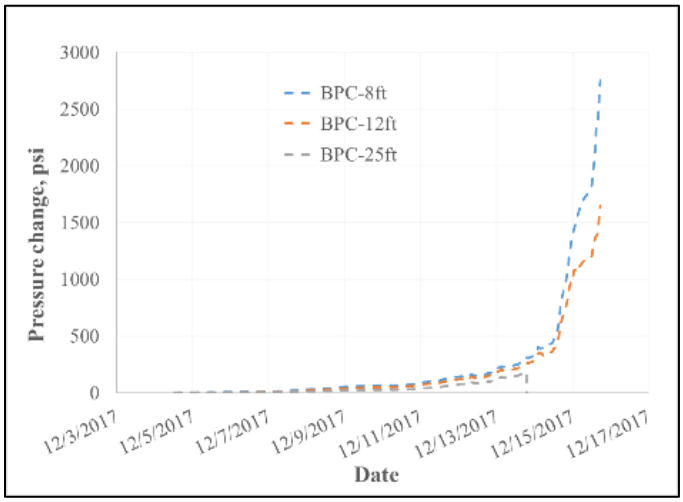

Figure 4. Pressure change in the BPCs for pillar -1 at site-2.

Roof Deformation/Sag

The vertical displacement of the immediate roof was examined via two 6-point roof extensometers (RXL and RXR) at each site; see Figure 2 for the location of the RXR and RXL extensometers. Figures 5 and 6 show the measured vertical displacement of the six-point roof anchors at site-1 and site-2, respectively. During retreat mining at site-1 the maximum and minimum anchor displacements are roughly 1.4 in (0.0355 m) and 0.6 in (0.0152 m). The RXR extensometer data was corrupted, it neither matches the results of the RXL nor our visual observations at the site. The RXR at 8 ft might have slipped or a crack in the rock layer might have caused that high displacement of that anchor. At site-2, the maximum and minimum anchor displacements are roughly 1.2 in (0.0304 m) and 0.6 in (0.0152 m), respectively.

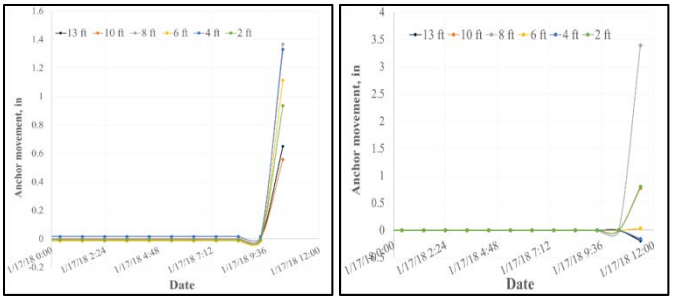

a. RXL b. RXR

Figure 5. Measured roof deformation by six-point roof extensometers at site-1 a) RXL and b) RXR.

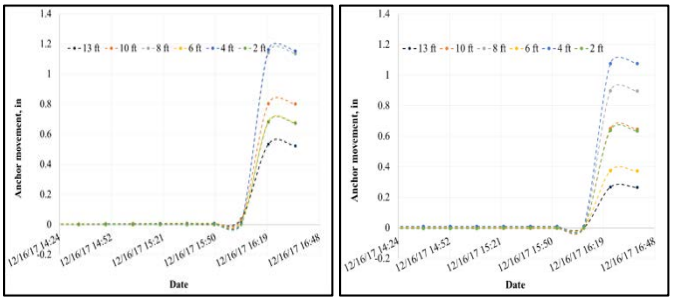

a. RXL b. RXR

Figure 6. Measured roof deformation by six-point roof extensometers at site-2 a) RXL and b) RXR.

Rib Deformation

The two main factors that lead to an increase risk of rib falls during retreat mining are thicker coal seams and higher stress levels. The Multi-Point Rib Extensometers (MPRX) were used to monitor the deformation of the rib for pillar-2. Figure 7 shows the rib deformation and anchors movement at specific locations inside instrumented pillar-2 for site-2. The MPRX results for site-1 was zero during mining at all anchor depths, followed by an instantaneous shift of 4 in (0.101 m) of movement, which is improbable compared to our visual observations at the time. It was not possible to determine if the movement of this MPRX was the result of an electronics malfunction or if it was struck by mobile mining equipment. Either possibility could explain the resulting displacement that was recorded.

LARGE-SCALE FLAC3D MODEL SETUP

Large-scale FLAC3D models were used to replicate the actual behavior of the coal/rock masses and to simulate the abutment loading and stress transfer due to pillar extraction at each site. With the proper input parameters, the predicted displacement and stresses from FLAC3D models are expected to be consistent with the field measurements and observations. The input parameters include material properties for coal/rock strata, gob properties, and the loading conditions. Since both sites are located in the same panel, the pillar sizes are roughly the same and the stratigraphic column at the two sites are similar, the same FLAC3D model geometry and lithology was used to simulate both site-1 and site-2. However, the overburden depth and the retreat plan are different at the two sites as explained previously. Also, the gob model for each site is different due to the poor caving characteristics exhibited at site-2 compared to site-1.

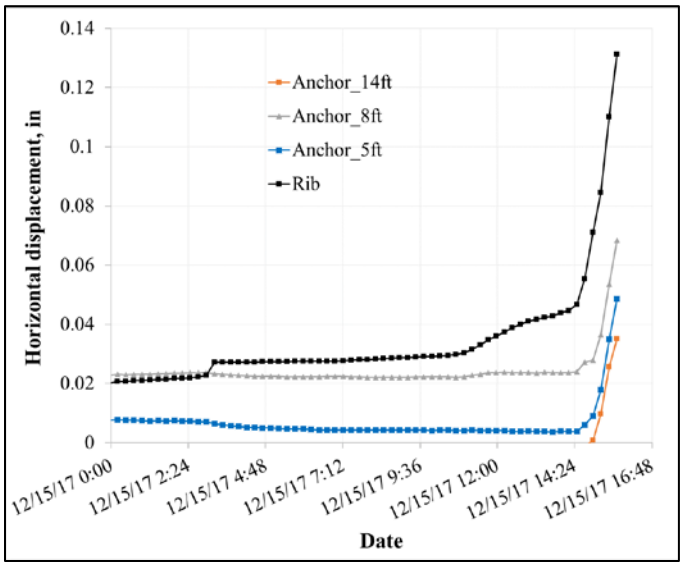

Figure 7. Measured rib deformation by MPRX for pillar-2 at site-2.

The dimensions of the large-scale FLAC3D models were determined to ensure stress transfer between the instrumented pillars and their surroundings: gob and unmined pillars. For each instrumented site, the dimensions of the model are 734 ft (224 m) x 1,102 ft (336 m) x 199 ft (60.6 m) in X, Y, and Z directions, respectively. The X and Y represent the horizontal plane, and the Z direction represents the vertical direction or depth. The roof and the floor strata were modeled using elastic material models because, based on our visual observations, the roof and floor strata were strong enough to withstand the development and abutment-induced stresses without noticeable failure. A pillar with dimensions 52.4 ft (16 m) x 98.4 ft (30 m) rib-to-rib was used as an approximation for all pillar sizes in the model. The coal-pillar is composed of shale and coal, the shale was modeled using the elastic-perfect plastic Mohr-Coulomb material model, and the coal was modeled using the coal-mass model developed by Mohamed et al. (2015). This coal-mass model considers the effect of face cleats in the coal material. The coal-mass model has the capability to capture the development of rib fractures in the coal material. The element size of the instrumented pillars in the large-scale FLAC3D models was 0.82 ft (0.25 m) x 0.82 ft (0.25 m) x 0.33 ft (0.10 m) in the X, Y, and Z directions, respectively.

Tables 4 and 5 summarize the material properties used in the large-scale FLAC3D models for rock and coal strata. The constitutive behavior of the gob material is expressed by strain-hardening behavior shown in equation-1 (Salamon, 1990). For site-1, where good caving characteristics were observed in the field, calibration of the gob material required reducing the maximum gob strain ( ) or increasing the initial Young's modulus (E_0). By trial and error, the that provided good agreement with the observed caving characteristics for site-1 was 0.09.

$$\sigma = \frac{E_0 \times \varepsilon}{1 - \frac{\varepsilon}{\varepsilon_m}} \qquad \textbf{Equation - 1}$$

Where:

σ = vertical gob stress,
E_0 = initial Young's modulus of 1,740 psi,
ε = vertical gob strain,
ε_m = maximum gob strain equal to 0.09 for site-1 and 0.33 for site-2.

LARGE-SCALE FLAC3D MODEL CALIBRATION

The visual observations and field instrumentation data collected at each site was used to calibrate the large-scale FLAC3D models. Initially, it was planned that data collection would continue until the instrumented pillars were fully extracted. Unfortunately, the wires connecting the instruments to the data logger were damaged or cut during the mining process when the pillar line was at the instrumented pillars. Figure 8 shows the loading conditions and the location of the pillar line with respect to the instrumented pillars (pillar-1 and pillar-2) at each site. The calibration process for the FLAC3D model was conducted by iterating the coal-mass scale and the fracture plastic shear strain to satisfy visual observations and instrumentation results at site-1. The best match was obtained when the coal-mass scale and the plastic shear strain were 20 and 0.01, respectively. The coal-mass scale and plastic shear strain determined from the calibration at site-1 were used in the FLAC3D model to simulate site-2 because these properties were not expected to change significantly from site to site in the same panel.

Table 4. Coal-mass material properties used in the model.

Coal-mass properties	
Young's Modulus, psi	3.9E5
Poisson's ratio	0.25
Intact compressive strength, psi	1,885
Coal-mass scale	20 .0
Fracture plastic shear strain	0.01
Fracture plastic tensile strain	0.001
Joint friction angle, degrees	25.0
Joint residual cohesion, psi	14.5
Joint residual tensile strength, psi	1.45
Joint degradation rate, psi/strain	1.15

Table 5. Rock-mass and interface material properties used in the model.

Rock properties					**Interface properties**	
Rock type	Young's Modulus, psi	Poisson's ratio	Cohesion, psi	Friction angle, degrees	Friction angle, degree	30.0
					Friction-residual, degree	14.0
Shale	2.2E6	0.30	652.5	25.0	Cohesion, psi	82.6
					Cohesion-residual, psi	50.7
Sandy shale	2.9E6	0.26			Tension, psi	16.0
Sandstone	3.62E6	0.23			Tension-residual, psi	0.0
Silty shale	2.9E6	0.26			Normal stiffness, psi/in	3.5E6
					Shear stiffness, psi/in	1.2E5

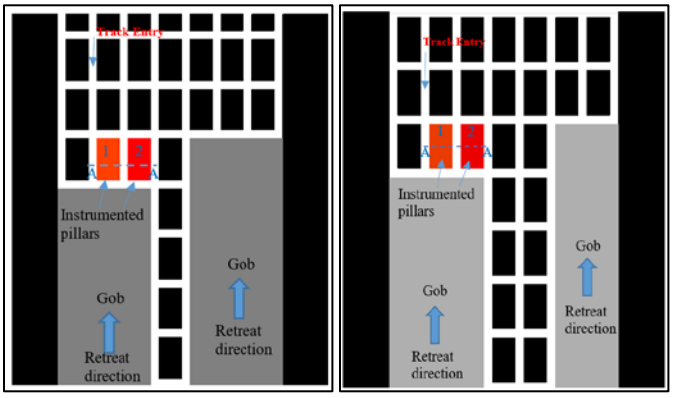

a. site-1 b. site-2

Figure 8. Loading conditions and pillar line locations at the two instrumented sites.

The large-scale FLAC3D model was calibrated based on the following:

1) Comparing the vertical stress from the BPCs at 8 ft (2.4 m), 12 ft (3.6 m), and 25 ft (7.6 m) inside instrumented pillars 1 and 2 at site-1 and site-2 with FLAC3D model results. Figures 9 and 10 show the results of the comparison for pillar-1 and pillar-2, respectively. For site-2, the borehole pressure cell at 25 ft (BPC–25ft) inside pillar-1 was damaged a few days after installation. The calculated vertical stress

from the FLAC3D model was obtained at cross-section AA (see Figure 8) at mid-pillar height for two loading conditions: development and abutment loading. The calculated vertical stress from the model (black profile) shows good agreement with the monitored vertical pressure from the BPCs for pillar-1 and pillar-2 at both sites.

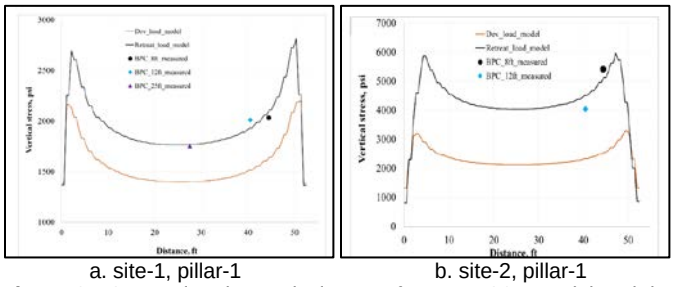

a. site-1, pillar-1 b. site-2, pillar-1

Figure 9. Comparing the vertical stress from FLAC3D model and the measured BPCs at cross-section A-A pillar -1 for a) site-1 and b) site-2.

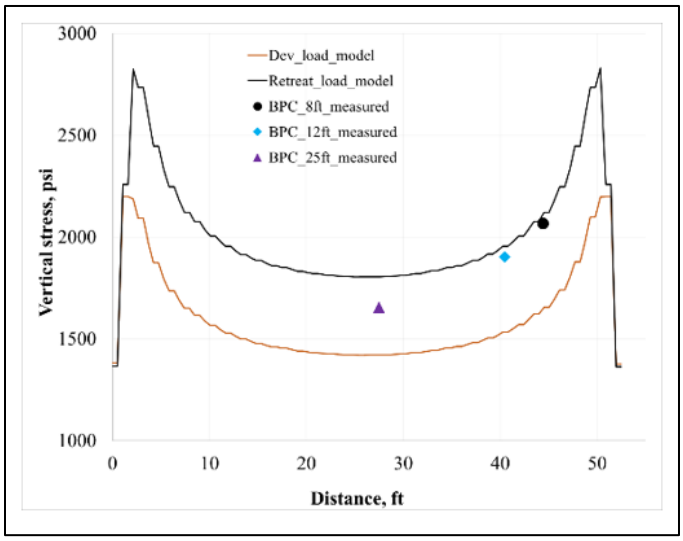

Figure 10. Comparing the vertical stress from FLAC3D model and the measured BPCs at cross-section A-A pillar-2 for site-1.

2) Comparing the rib sloughing in the FLAC3D model with visual observations. For the loading condition shown in Figure 8, based on the visual observations, the observed rib sloughing at the instrumented site-1 was less than 1.0 ft (0.3 m), while for site-2 it did not exceed 2.0 ft (0.6 m) at the side of the pillar. Based on the FLAC3D model for site-1, the depth of fracture—which is an estimate for the rib sloughing—from the model is zero at the sides of the instrumented pillars, while it is 1.64 ft (0.5 m) at the corners. For site-2, the depth of fracture is 1.64 ft (0.5 m) at the sides of the pillar (see Figure 11). However, at the pillar corner, the depth of fracturing exceeds 1.64 ft (0.5 m). Generally speaking, the FLAC3D models provide acceptable agreement with the observed rib sloughing at site-1 and site-2.

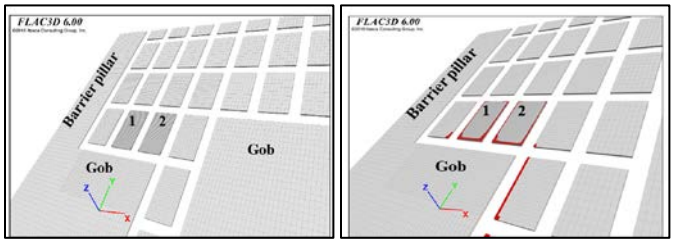

a. Site-1 b. Site-2

Figure 11. Calculated rib sloughing (red zones) for instrumented pillars 1 and 2 at a) site-1 and b) site-2.

3) Comparing the vertical roof displacement in FLAC3D with visual observation and instrumentation results. The visual observation showed small roof deformations at both site-1 and site-2. Based on the instrumentation results, the average vertical movement of the immediate roof due to pillar retreat was approximately 1.0 in (24.5 mm) and 0.9 in (22.8 mm) at site-1 and site-2, respectively. The FLAC3D model shows that the roofline moved approximately 0.22 in (5.6 mm) and 0.72 in (18.3 mm) at site-1 and site-2, respectively, after deducting the vertical displacement due to development loading (see Figure 12). The displacement from the FLAC3D model is the summation of the movement due to development and retreat mining loading conditions. There is a good agreement between the instrumentation results and the model results at site-2, while at site-1 the model provides some agreement with the instrumentation results.

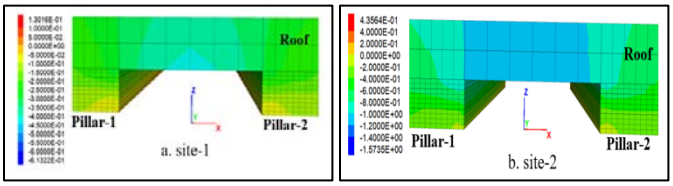

Figure 12. Vertical displacement (in inches) of the immediate roof from FLAC3D at a) site-1 and b) site-2.

MAXIMUM SHEAR DISPLACEMENT (ROOF SHIFT) AT THE DEEP SITE

Currently, the mine is using five 4-ft (1.2-m) #6 (6/8-in), grade 60, fully grouted, nontensioned rebar bolt per row as the primary roof support in areas with a depth of cover greater than 1,000 ft (304.8 m), while in shallower areas the same configuration with #5 (5/8-in) rebar is used. The mine is considering using the #5 rebar bolt at both deep and shallow cover areas, but there is some concern with the reduction in lateral load capacity of the smaller diameter bolt. Because, in some cases, fatalities that have occurred during pillar recovery reported shear failure of #5 (5/8-in) fully grouted rebar bolt in deep-cover room-and-pillar retreat mines (NIOSH, 2010). To examine if the #5 (5/8-in) rebar bolt could be used at the +1,000 ft (304.8 m) depth of cover in the study mine, the calibrated large-scale FLAC3D model was used to predict the induced shear displacements (roof shifting) in the bolted horizon during the retreat of instrumented pillars (pillar-1 and pillar-2) and the adjacent pillar. The instrumented pillars and the adjacent pillar were mined in three stages (see Figure 13). For the first stage, retreat-1, the instrumented pillar-2 and half of pillar-1 were mined. For the second stage, retreat-2, three-quarters of pillar-1 and one-quarter of the adjacent pillar were mined. For the third stage, both instrumented pillars and adjacent pillar were completely mined. The induced maximum shear displacement within the yellow box where miners were likely to be exposed was determined from these three stages (see Figure 13). As shown in Figure 14 the induced maximum shear displacement was found to be approximately 1/8 in (3.2 mm), which matches with the scope observations conducted by the mine.

ASSESSING THE CAPACITY OF #5 AND #6 REBAR BOLT GRADE 60 AT SITE-2

The first question usually asked about roof bolts is: “what is its capacity?” two types of capacities are known for roof bolts: yield and ultimate. These can be calculated from the diameter of the bolt and the properties of the steel. The yield and ultimate strengths of grade 60 steel is 60,000 psi (413 MPa) and 90,000 psi (620 MPa), respectively. Studies conducted by Signer (2000) on instrumented bolts have shown that 75 % of the instrumented bolts reached the yield limit of the steel, and 50 % of the bolts exceeded the yield point. On one hand, this might give a hint that the bolt capacity could be calculated based on the ultimate strength of the steel. However, these values obtained by Signer include a variety of loading conditions, most of which represent the abutment loading from the second passage of the longwall. On the other hand, Mark (2000) used the yield strength of the bolt to estimate the support capacity of the roof bolt system for use in the Analysis of Roof Bolt Systems (ARBS). Colwell (2006) used the shear strength of the bolt to estimate the bolt capacity for coal pillar ribs. Wagner (1985) claimed that the shear strength of bolt is 50% of the ultimate tensile

strength. In this study, since there is some uncertainty about the ground conditions/roof properties in the bolted horizon in addition to the uncertainty about the loading conditions due to variable gob caving characteristics, it is prudent to design the capacity of roof bolt systems based on the yield strength rather than the ultimate strength.

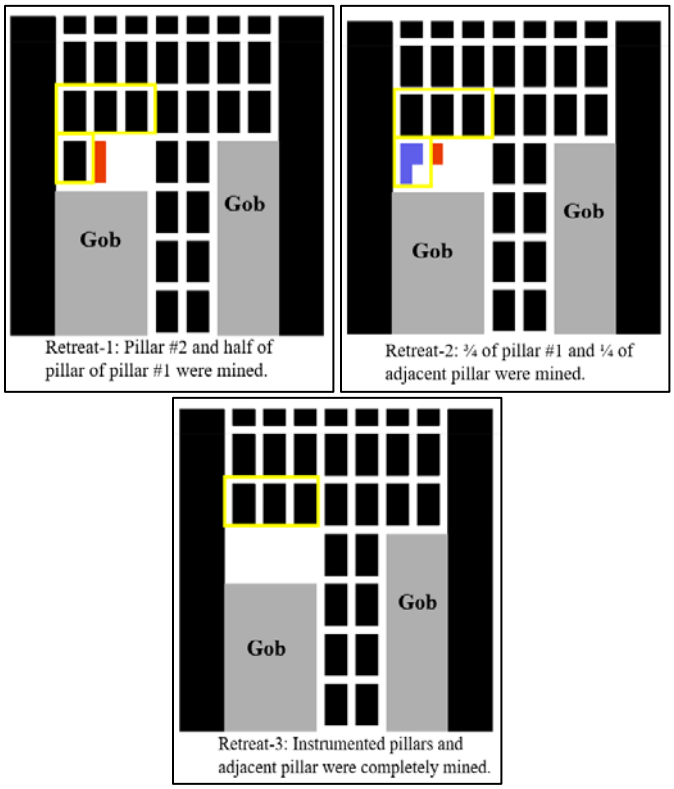

Figure 13. Maximum shear displacement was obtained from the worst-case scenarios.

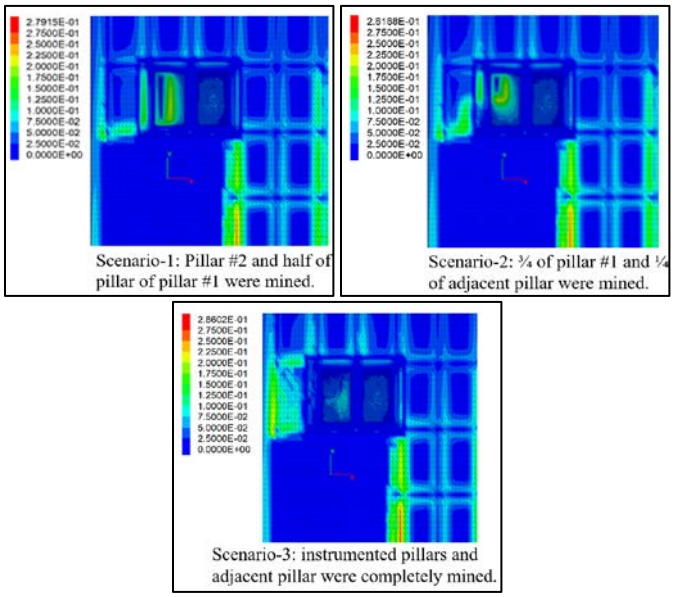

Figure 14. FLAC3D induced shear displacement (in inches) for three scenarios of pillar retreat mining.

A small-scale FLAC3D model was generated to calculate the induced axial stresses in the 4-ft (1.2-m) #5 (5/8-in) and 4-ft (1.2-m) #6 (6/8-in) fully grouted rebar bolts when they are subjected to both an axial load of 2.9 tons (2.6 metric ton) and a roof shift of 1/8 in (3.2 mm). The 2.9-ton vertical load was used to simulate a detached rock-block from the immediate roof of size 3.5 ft (1.0 m) x 3.5 ft (1.0 m) x 3.0 ft (0.9 m), assuming the unit weight of the rock is 159 lb/ft^3. The small-scale FLAC3D model consists of two identical rock-blocks of size 4.0 ft (1.2 m) x 4.0 ft (1.2 m) x 4.0 ft (1.2 m). The bolt is grouted at the center of the blocks. One-third of the bolt is grouted in the top block, and the remaining portion of the bolt is grouted into the bottom block, see Figure 15.

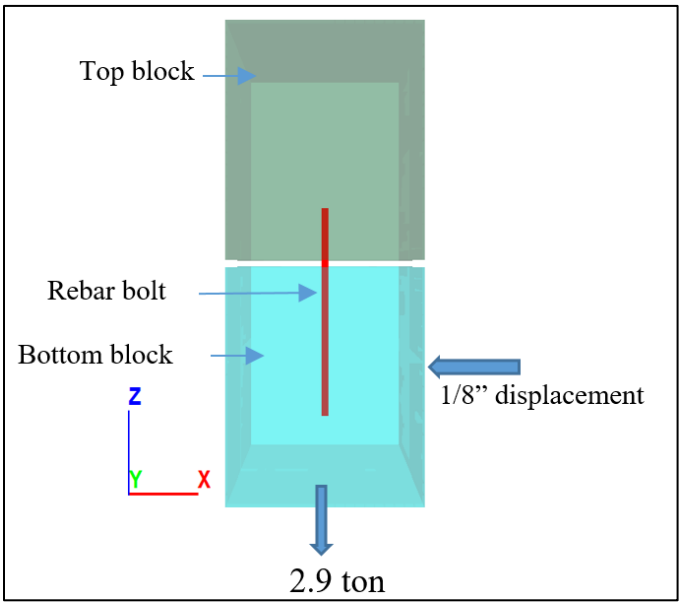

Figure 15. Schematic of the fully grouted bolt model from FLAC3D.

Modified pile structural elements in FLAC3D were used to simulate the bending resistance of the bolt and the strain-softening behavior of the grout. The pile structural elements interact with the FLAC3D grid via normal and shear coupling springs. Geometric, material, and coupling-spring properties of the pile structural elements used to simulate the bolt are shown in Table 6 (Esterhuizen, 2018).

Table 6. Grout and bolt properties used in FLAC3D model.

Young's modulus, psi	2.90E7
Poisson's ratio	0.30
Second moment of inertia, in^4	0.0075
Polar moment of inertia, in4	0.0150
Coupling-cohesion-normal, lbf/in	1,000
Coupling-stiffness-normal, lb/in2	145,112
Coupling-stiffness-shear, lb/in2	145,112
Coupling-cohesion-shear, lb/in	1,605
Cross-sectional area for #5 bolt, in2	0.307
Cross-sectional area for #6 bolt, in2	0.442
Hole diameter, in	1.0

The model was solved in two steps: in the first step the bolt was pulled by a 2.9-ton (2.6 metric ton) vertical load applied on the bottom block. In the second step a horizontal displacement of 1/8 in (3.2 mm) was applied on the lower block to simulate the roof shifting. The induced axial stresses after the second stage of loading in #5 (5/8-in) and #6 (6/8-in) bolts due to vertical and horizontal movements are obtained from FLAC3D models. A commonly observed phenomenon is the S-shaped shown in Figure 16 resulted from axial and bending stresses. The safety factor based on the yield strength was calculated for both #5 (5/8-in) and #6 (6/8-in) diameter grade 60 bolts, as follows:

$$SF(yield) = \frac{Induced\ axial\ stress}{60{,}000} \qquad \textbf{Equation -2}$$

Based on the model results, the safety factor based on the yield strength for #6 (6/8-in) rebar bolt is 2.47. No safety factor was calculated for the #5 (5/8-in) rebar bolt because the bolt already exceeded its yield limit. The Given uncertainty of the geological conditions, roof separation, and roof shifting from place to place in the

study mine, it was not recommended to use the #5 (5/8-in) rebar bolt at site-2 where the depth of cover is equal to or greater than 1,500 ft (457.3 m).

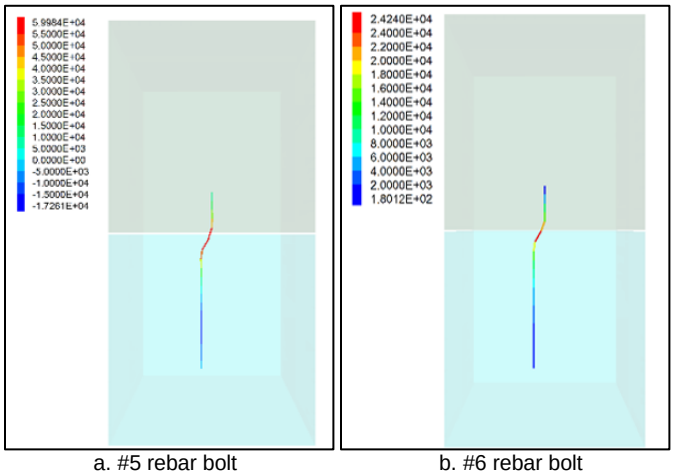

a. #5 rebar bolt b. #6 rebar bolt

Figure 16. Induced axial stresses in psi for a) #5 (5/8-in) rebar bolt and b) #6 (5/8-in) rebar bolt from FLAC3D.

VERIFICATION OF THE FLAC3D BOLT MODEL

The small-scale FLAC3D bolt model was verified by examining the safety factor of the #5 (5/8-in) rebar bolt at site-1. The mine is using the #5 rebar bolt when the overburden depth is less than 1,000 ft (304.8 m) without any noticeable roof bolt problems. At 1,000 ft (304.8 m) of cover, the induced maximum shear displacement obtained for the three scenarios shown in Figure 12 is approximately 1/16 in (1.8 mm). A small-scale FLAC3D bolt model was generated similar to that shown in Figure 15 except that the applied horizontal displacement was 1/16 in (1.8 mm). The calculated safety factor based on the yield strength for the #5 (5/8-in) rebar bolt is 1.1 and 1.65 based on the ultimate strength. The strain in the # 5 simulated bolt is less than the yield strain of the steel (0.2% strain) and way below the fracture strain of the steel (9% strain). Hence, the FLAC3D bolt model was confirmed by field observations at site -1. Based on the two calibrated small-scale FLAC3D models, #5 (5/8-in) rebar should not be used if the depth of cover exceeds 1,000 ft (304.8 m).

CONCLUSION

This paper presents the in-situ monitoring and numerical modeling results for two deep-cover room-and-pillar retreat mining sites the depth of cover for the two sites are 1,000 ft (304.8 m) and 1,500 ft (457.3 m), respectively. Large-scale FLAC3D models were calibrated based on visual observations and in-situ monitoring at the two sites. The calibrated models were able to replicate the coal/rock response in terms of deformation and stresses at the two sites. The models provided relatively good agreement between stresses and displacements when compared to both field observation and instrumentation results. These large-scale models were then used to assess roof bolt performance at the study mine.

The calibrated large-scale models were used to determine the maximum lateral displacement/ roof shifting due to pillar retreat mining at the two sites. Calibrated and validated FLAC3D bolt models were generated to examine the safety factor of the #5 (5/8-in) and #6 (6/8-in) rebar bolts grade 60 at 1,000 ft (304.8 m) and 1,500 ft (457.3 m) of cover at the study mine. Based on the model results and the geological conditions of the mine, the safety factor of the #6 (6/8-in) rebar bolt is 2.47, while the #5 (5/8-in) rebar bolt exceeded the yield limit of the steel at the deep-cover site.

The types of numerical models presented in this paper provide realistic simulations of stresses and displacements that can occur during pillar retreat mining. Additionally, the large-scale models presented here can be used to provide input data for small-scale models to analyze more specific behaviors such as rock/support interaction. These models can assist mine engineers in reducing the impact of elevated stresses when designing mine layouts, also they can help miners to select the appropriate bolts for reducing roof falls in future mining areas.

DISCLAIMER

The findings and conclusions in this paper are those of the authors and do not necessarily represent the views of the National Institute for Occupational Safety and Health (NIOSH).

REFERENCES

Chase E. F., Mark C., and Heasley A. K. (2002) “Deep cover pillar extraction in the U.S. coalfields.” In: Peng S. S, Mark C., Khair A.W., and Heasley K. A, eds. Proceedings of the 21st International Conference on Ground Control in Mining. Morgantown, WV: West Virginia University, pp. 68–80.

Colwell M. G. (2006) “A study of the Mechanics of coal mine rib deformation and rib support as a basis for engineering design.” Ph.D Thesis, Mining engineering, University of Queensland.

Esterhuizen G. S. (2018) personal communications.

Klemetti T. M., Sears M. M., and Tulu I. B. (2017). “Design concerns of room and pillar retreat panels.” Int. J. Min Sci. Technol. 27(1), pp.29–35.

Larson M. K., Tesarik D. R., Seymour J. B., and Rains R. L. (2000). “Instruments for monitoring stability of underground openings.” Proceedings: New technology for coal mine roof support. Mark C., Dolinar D.R., Tuchman R. J., Barczak T.M., Signer S. P., and Wopat P. F., eds. Cincinnati, OH: U.S. Department of Health and Human Services, Public Health Service, Centers for Disease Control and Prevention, National Institute for Occupational Safety and Health, DHHS (NIOSH) Publication No. 2000-151; (IC 9453). pp. 253–269.

Mark, C. (2000). “Design of roof bolt systems.” In proceedings: New Technology for Coal Mine Roof Support, ed. By C. Mark, D. R. Dolinar, R.J. Tuchman, T.M. Barazak, S.p. Signer, and P.F. Wopat. NIOSH Information Circular 9453, pp. 111-131.

Mark, C. (2009). “Deep cover pillar recovery in the US.” In: Proceedings 28th international conference on ground control in mining. Morgantown. pp. 1–9.

Mohamed, K.M., Tulu, I.B., and Klemetti, T. (2015). “Numerical Simulation of Deformation and Failure Process of Coal-Mass,” Proceedings of the 49th US Rock Mechanics/Geomechanics Symposium, Alexandria, VA, American Rock Mechanics Association.

MSHA. (2018). Part 50 Data User’s Handbook. Fatalities data. http://www.msha.gov/STATS/PART50/p50y2k/p50y2k.HTM, U.S. Department of Labor, Mine Safety and Health Administration (MSHA).

NIOSH (2010). “Research Report on the Coal Pillar Recovery under Deep Cover.” P. 79. U.S. Department of Health and Human Services, Centers for Disease Control and Prevention, National Institute for Occupational Safety and Health (NIOSH), Office of Mine Safety and Health Research (OMSHR).

Rashed G., Barton T., Sears M., Van Dyke M., and Mohamed K. (2018). “Estimation of the intact strength of coal using indirect methods.” In: Proceedings of the 37th International Conference on Ground Control in Mining. Morgantown, WV: West Virginia University, pp. 294–301.

Salamon M.D.G., 1990, “Mechanics of Caving in Longwall Coal Mining,” Proceedings of the 31st U.S. Symposium on rock mechanics, Colorado School of Mines, Golden, CO, pp 161-168. Mark, C. Deep cover pillar recovery in the US. In: Proceedings 28th international conference on ground control in mining. Morgantown; 28–30 July 2009. pp. 1–9.

Signer S. P. (2000). “Load behavior of grouted bolts in sedimentary rocks.” In proceedings: New Technology for Coal Mine Roof Support, ed. By c. Mark, D. R. Dolinar, R.J. Tuchman, T.M. Barazak, S.p. Signer, and P.F. Wopat. NIOSH Information Circular 9453, pp. 73-80.

Thomas W. R. (2015). “Development of a Wireless Borehole Extensometer for Monitoring Convergence in Underground Mines.” Master thesis, Virginia Tech, Mining & Minerals Engineering, pp. 93.

Wagner, H. (1985). Design of roof bolting patterns. Chamber of Mines workshop on roof bolting in collieries. Republic of South Africa. Johannesburg.

Zipf R. K. (2006). “Numerical modeling procedures for practical coal mine design.” Proceedings of the 41st U.S. Rock Mechanics Symposium, Golden, Colorado, June 17-21, 2006. Alexandria, VA: American Rock Mechanics Association, pp.1-11.